Electronic Supplementary Material (ESI) for Physical Chemistry Chemical Physics.

Supporting Information

Interfacial Properties of Borophene Contacts with Two-dimensional Semiconductors

Jie Yang, [1] Ruge Quhe[1,*], Shenyan Feng, [1] Qiaoxuan Zhang, [1] Ming Lei, [1,*] and Jing Lu [2, 3, *]

[1]State Key Laboratory of Information Photonics and Optical Communications and School of Science, Beijing University of Posts and Telecommunications, Beijing 100876, P. R. China
[2]State Key Laboratory for Mesoscopic Physics and Department of Physics, Peking University, Beijing 100871, P. R. China
[3]Collaborative Innovation Center of Quantum Matter, Beijing 100871, P. R. China

*Corresponding author: quheruge@bupt.edu.cn; mlei@bupt.edu.cn; jinglu@pku.edu.cn

1. Comparison of vdW-DF and vdW-D2 corrections

To estimate the effects of applying different vdW correction methods, we compared the optimized geometry and electronic properties of the β_{12} boro/MoS_2, β_{12} boro/graphene and β_{12} boro/black phosphorene as candidates to compare DFT-D2 and DFT-DF methods. By the correction of DFT-D2, the interlayer distances of the optimized geometries of these heterostructures are 3.17, 3.25, and 3.02 Å respectively, overall similar to the results (3.28, 3.45, 3.21 Å respectively) of DFT-DF correction. As shown in Figure R2, The characteristic bands of MoS_2 and graphene are identifiable, suggesting slight degree states overlapping with borophene. The size difference of the band gap of β_{12} boro/MoS_2 and β_{12} boro/graphene is less than 10% between two vdW correction methods. The black phosphorene under β_{12} borophene are metalized due to the strong band hybridization under both vdW corrections. Therefore, we believe that the key electronic structure features of the checked heterostructures are not sensitive to different methods of vdW treatment.

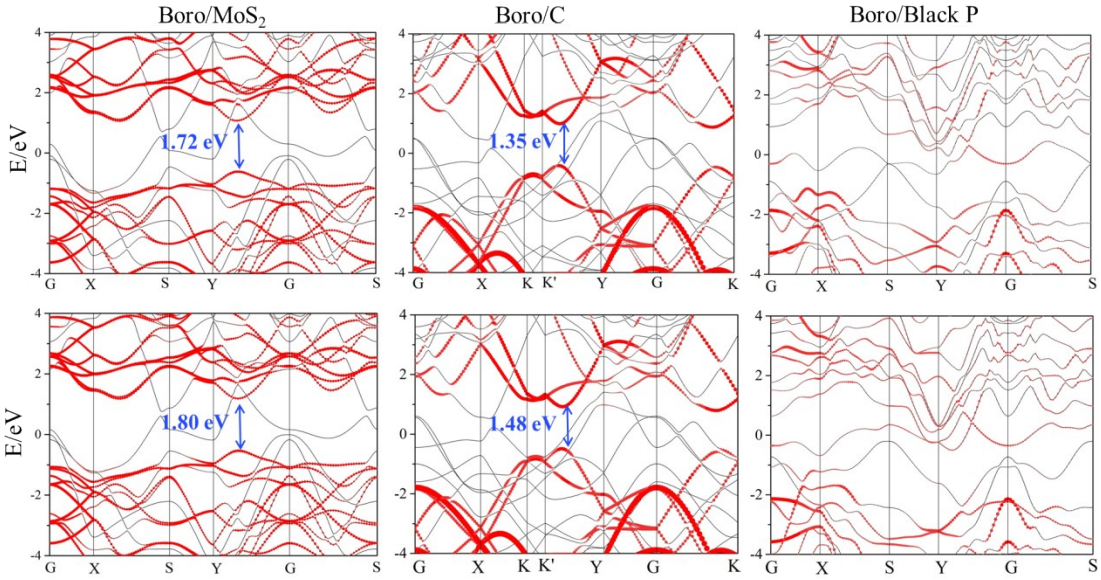

Figure S1. Band structures of β_{12} boro/MoS_2, β_{12} boro/C and β_{12} boro/Black P with different vdW corrections. The top alignment is calculated with DFT-DF. The bottom alignment is calculated with DFT-D2.

2. Molecular Dynamics Calculations

The dynamical stability of the Δ boro/2D semiconductor systems is studied by molecular dynamics (MD) simulations. MoS_2, graphene and black phosphorene are chosen as candidates of MX_2, group IV and group V-enes. The simulations are performed in 1 ps time scale at room temperature (300 K).

The geometrical structure of Δ boro/MoS_2 after MD simulation shows no significant changes compared with the optimized structure. Black phosphorene with slight distortion but recognizable structure moves closer to deformed triangular borophene. Significant distortion is foundin Δ boro/C. The temperature of Δ boro/MoS_2 and Δ boro/ black phosphorene tends to slightly fluctuate about 300K. The energy of Δ boro/MoS_2 and Δ boro/ black phosphorene tends to ~ -43.22 eV and ~ -182.21 eV respectively. However, curves of temperature and energy versus time of Δ boro/graphene lead to violent oscillations. The range of temperature is approximately 100~600 K, while the energy changes from -136.93 eV to -4.96 eV.

In terms of the structure change and fluctuation range of temperature and energy versus time, Δ boro/MoS_2 and Δ boro/ black phosphorene prove relatively good stability, while Δ boro/graphene lacks of stability.

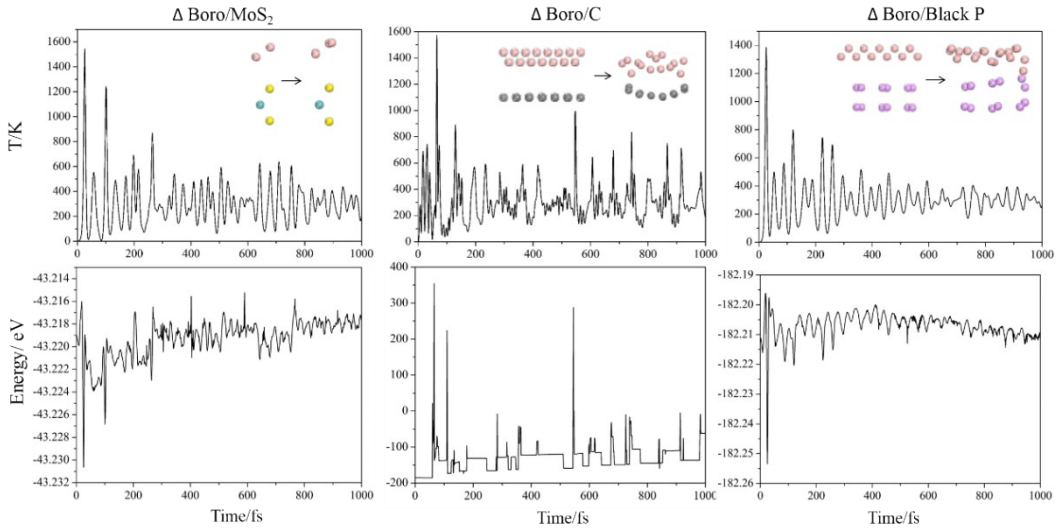

Figure S2. Changes of temperature versus time (top panel) and changes of energy versus time (bottom panel) obtained from molecular dynamics simulation of triangular borophene/MoS_2, C and Black P contacts. The inserted structures are comparison of the geometry of the heterostructures before (left) and after (right) the molecular dynamical simulations.

3. Interfacial Properties of Δ Borophene/2D Semiconductor

Table S1. Calculated interfacial properties of monolayer Δ boro/2D material contacts.

		ε / %	d_z / Å	$\Phi_{\perp}$/eV			$\Phi_{//}$ /eV	
				Φ_{TB}	$\Phi_{\perp}^{e}$	$\Phi_{\perp}^{h}$	$\Phi_{//}^{e}$	$\Phi_{//}^{h}$
	MoS_2	1.31	3.11	0	1.53	0	1.55	0.30
Δ Boro/	$MoSe_2$	0.36	2.94	0	0.89	0	1.21	0.20
MX_2	WS_2	1.38	3.14	0	1.80	0	1.55	0.30
	WSe_2	0.38	2.98	0	1.15	0	1.45	0.20
	C	0.59	3.36	0	--	--	--	--
Δ Boro/	Si	0.79	2.01	0	--	--	--	--
IV-ene	Ge	2.19	1.57	0	--	--	--	--
	Sn	1.62	2.18	0	--	--	--	--
	Blue P	0.44	2.37	0	0	0	0.44	1.56
Δ Boro/	Black P	1.45	3.28	0	1.34	0	--	0
V-ene	As	1.72	3.41	0	0.95	0	--	0
	Sb	2.13	2.28	0	0	0	--	0

In order to diminish lattice mismatch of Δ borophene/2D semiconductors as small as possible, the supercell matching patterns are set as follows: (2×1) Δ boro/(1×1) MX_2 (M = Mo, W; X = S, Se) , (7×1) Δ boro/(3×1) C, (4×4) Δ boro/(3×1) Si, (7×1) Δ boro/(2×1) Ge, (3×3) Δboro/(2×1) Sn, (2×1) Δ boro/(4×1) blue P, (5×2) Δ boro/(3×1) black P, (4×2) Δ boro/(1×3) As and (7×1) Δ boro/(1×2) Sb. The lattice mismatches between layers of the above heterostructures are among 0.36% – 2.19%.

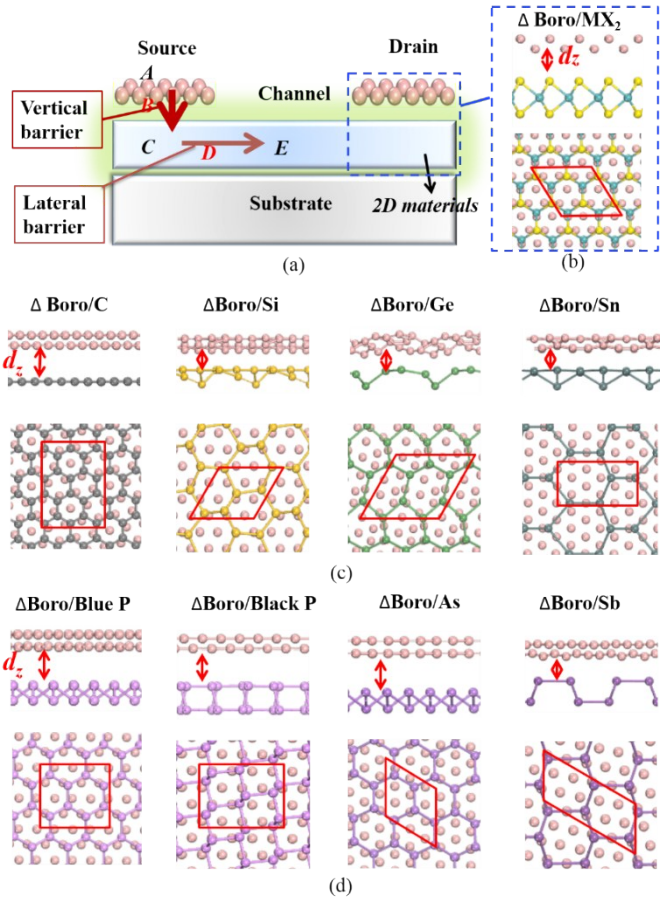

Figure S3. (a) Optimized structures of the Δ boro/2D semiconductor top atomic contacts. Side and top views of the most stable configurations: (b) Δ borophene contact to MX_2 (M = Mo, W; X = S, Se); (c) Δ borophene contacts to the group IV-enes; (d) Δ borophene contacts to the group V-enes.

The key properties of the 12 interfaces of Δ borophene/2D semiconductor are summarized in Table S1. In all the checked cases, vanished tunnel barrier and p-type Schottky barrier along the vertical direction are achieved, as shown in Figure S4-S8. With such low barriers and highly hybrid orbital, metallized Δ borophene contacted silicene, germanene, stanene, black phosphorene, arsenene and antimonene transistors, whose ρ_m exceeds 0.10 $Å^{-3}$, are expected for especially high carrier injection efficiency.

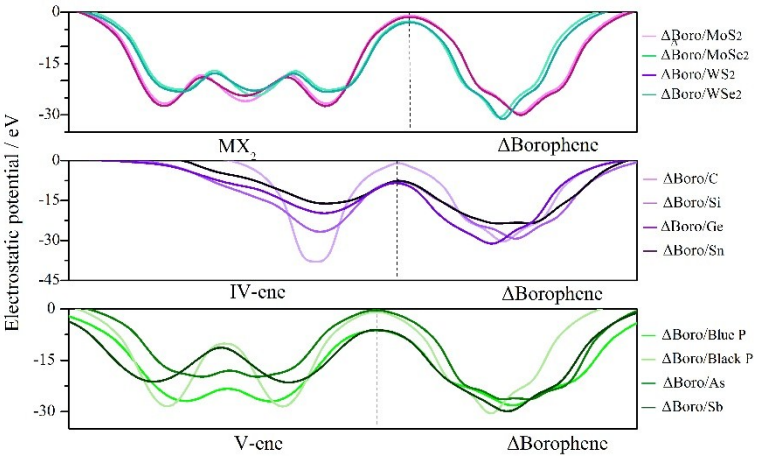

Figure S4. The averaged electrostatic potential versus *z* position for Δ boro/2D material contacts. The Fermi level is set at zero.

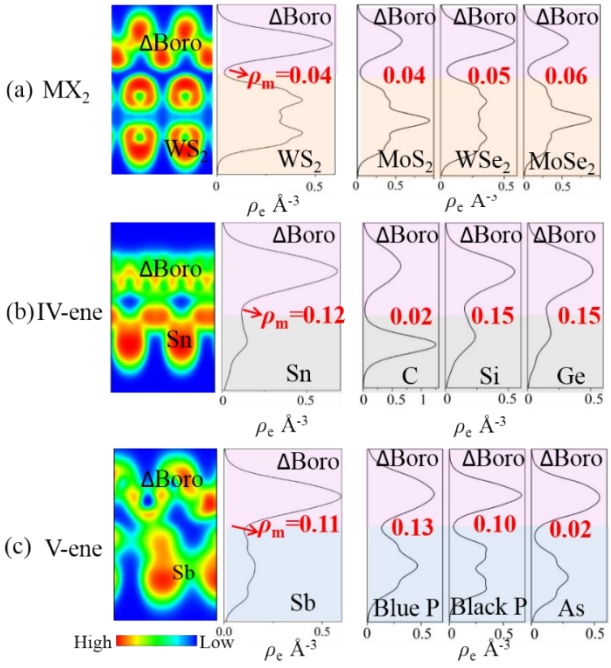

Figure S5. Charge density of Δ boro/2D material contacts: (a) Δ boro/MX_2, (b) Δ boror/group IV-enes, (c) Δ boro/group V-enes. ρ_e is the average electron density value in *x*-*y* plane. ρ_m in each row indicates the minimum value of the average electron density in the physical separation district of interfacial configurations.

Since the Schottky barrier is absent along the vertical direction in all the checked Δ boro/2D contacts, we further check the existence of the Schottky barrier along the lateral direction. In Figure S9, the lateral SBH is for holes $\Phi_{//}^{h}$ between Δ boro/MX_2 and the channel MX_2 are 0.2 ~ 0.3 eV. The lateral SBHs of Δborophene contacted group V-enes vary:

black phosphorene, arsenene and antimonene: $\Phi_{//}^{h}$ = 0 eV; blue phosphorene: $\Phi_{//}^{e}$ = 0.4 eV. It is noted that the estimation of the lateral Schottky barrier here do not consider the interaction between the electrode and channel regions, and a transport simulation with inclusion of the electrode-channel coupling is desirable to obtain more precise values.

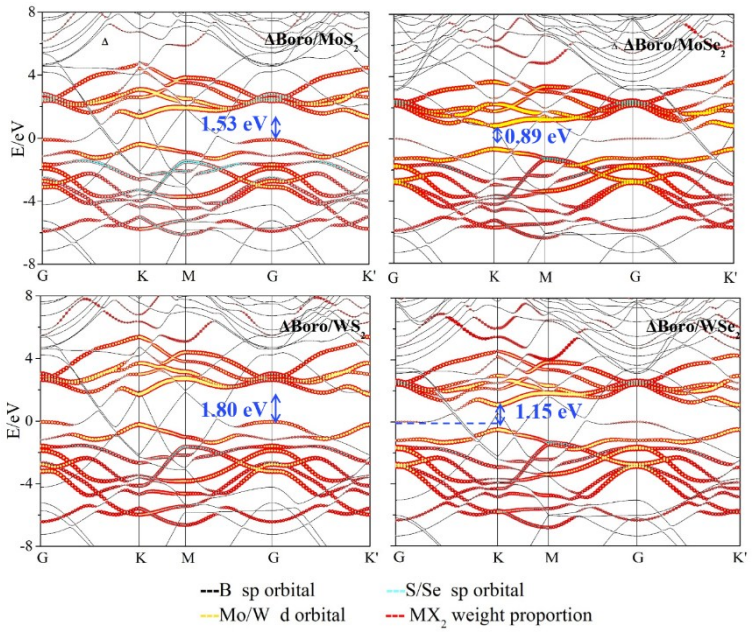

Figure S6. Band structures of the Δ boro/MX_2 interfaces. The black lines are the band structures of the interfacial system; the red lines correspond to the contribution from MX_2 with the line width proportional to the weight.

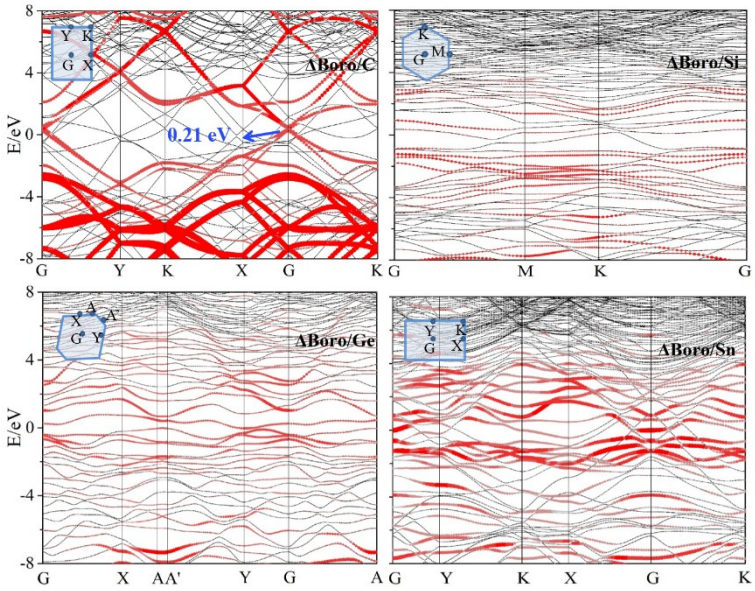

Figure S7. Band structures of the Δ boro/group IV-enes. The black lines are the band structures of the interfacial system; the red lines correspond to the valid contribution from group IV-enes; the line width is proportional to group IV-enes' weight.

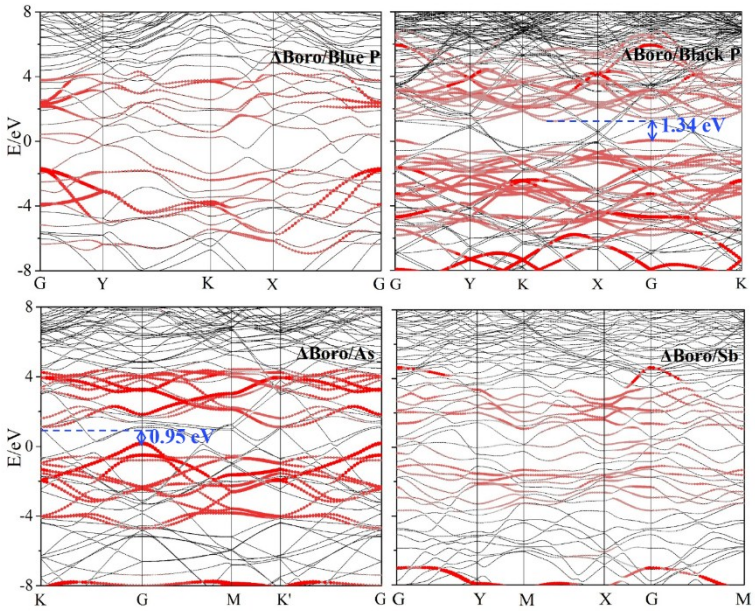

Figure S8. Band structures of the Δ boro/group V-enes. The black lines are the band structures of the interfacial system; the red lines correspond to the contribution from group V-enes after interaction with Δ borophene with the line width proportional to the weight. The Fermi level is set at zero.

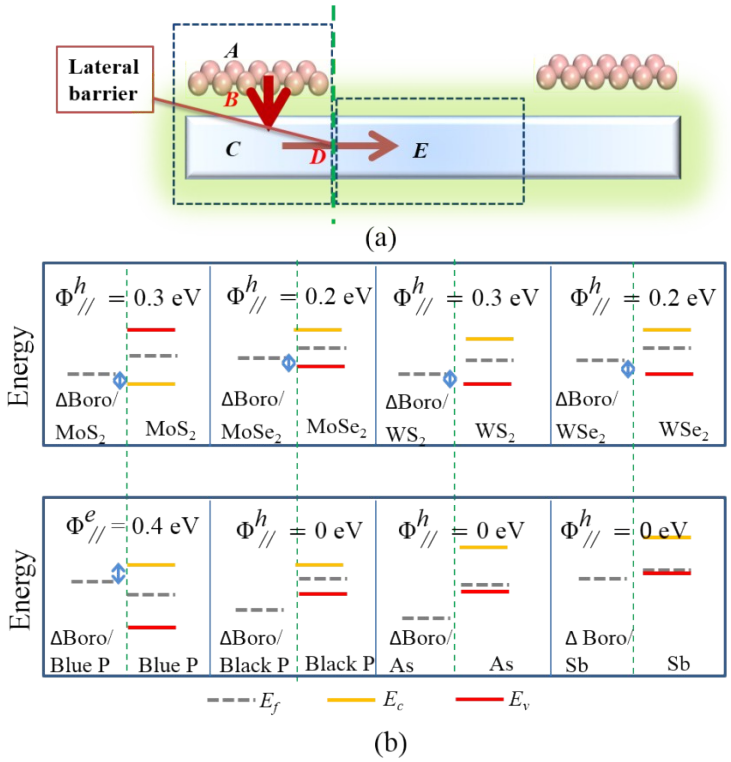

Figure S9. (a) Lateral Schottky barrier from the Δ boro/2D material contact to the 2D material

in channel (*C*→*D*→*E*); (b) Band alignments between the Δ boro/2D material heterostructure and 2D material.

To summarize the interfacial properties of the Δ borophene contacts to different 2D materials and evaluate these contacts for device applications, we divide the contacts into different types by taking account of the vertical barrier, lateral barrier, and the orbital overlap. Since the vertical barrier in all the checked cases are zero, we only provide the values of the average interfacial electron density ρ_m and the lateral barrier in Figure S10. The Δ borophene contacts to the 2D semiconductor with sizable bandgaps (MX_2 and group V-enes) are classified into 3 types: type I, low lateral barriers, and some degree of orbital overlapping; type II, low lateral barrier and strong orbital overlap; type III, high lateral barrier and highly hybrid orbital. Likewise, the Δ borophene contacted group IV-enes with very small bandgaps are classified into two types: type I' with lower degree of orbital overlapping and type II' with highly hybrid orbital.

Apparently the type II and type II' contacts allow the highest efficiency of carrier injection and are most desirable. High drain currents are expected in the black phosphorene,

arsenene, antimonene, silicene, germanene and stanene transistors with Δ borophene electrodes, since their small lateral barriers and highly hybrid orbital. Contact optimization method is needed if Δ borophene is used as electrode for blue phosphorene transistors as they suffers a big Schottky barrier along the lateral direction. As for the Δ borophene contacted MX_2 and graphene, no Schottky barrier occurs in both vertical and lateral directions and the main obstacle is the relatively weak orbital overlapping.

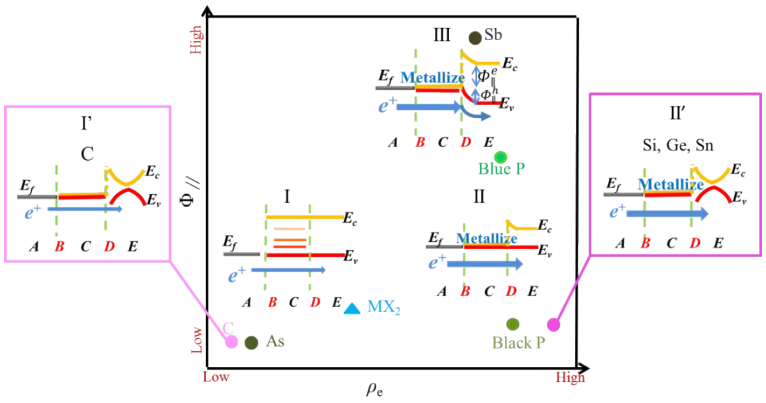

Figure S10. Different types of band diagrams in the Δ borophene contacted transistors. E_f is the Fermi level, E_c and E_v are conductive and valence bands of the 2D semiconductors.